Modulation of Calcium Current in Arteriolar Smooth Muscle by $\alpha_v\beta_3$ and $\alpha_5\beta_1$ Integrin Ligands

Xin Wu,* Jon E. Mogford,* Steven H. Platts,* George E. Davis,‡ Gerald A. Meininger,* and Michael J. Davis*

*Microcirculation Research Institute and Departments of Medical Physiology, ‡Pathology and Laboratory Medicine, Texas A & M University Health Science Center, College Station, Texas 77843-1114

Abstract. Vasoactive effects of soluble matrix proteins and integrin-binding peptides on arterioles are mediated by $\alpha_v\beta_3$ and $\alpha_5\beta_1$ integrins. To examine the underlying mechanisms, we measured L-type Ca^{2+} channel current in arteriolar smooth muscle cells in response to integrin ligands. Whole-cell, inward Ba^{2+} currents were inhibited after application of soluble cyclic RGD peptide, vitronectin (VN), fibronectin (FN), either of two anti–β_3 integrin antibodies, or monovalent β_3 antibody. With VN or β_3 antibody coated onto microbeads and presented as an insoluble ligand, current was also inhibited. In contrast, beads coated with FN or α_5 antibody produced significant enhancement of current after bead attachment. Soluble α_5 antibody had no effect on current but blocked the increase in current evoked by FN-coated beads and enhanced current when applied in combination with an appropriate IgG. The data suggest that $\alpha_v\beta_3$ and $\alpha_5\beta_1$ integrins are differentially linked through intracellular signaling pathways to the L-type Ca^{2+} channel and thereby alter control of Ca^{2+} influx in vascular smooth muscle. This would account for the vasoactive effects of integrin ligands on arterioles and provide a potential mechanism for wound recognition during tissue injury.

Key words: voltage-gated Ca^{2+} channel • vascular smooth muscle • wound repair • extracellular matrix • integrin-mediated signaling

INTEGRINS are heterodimeric receptors (α, β) that mediate cell–extracellular matrix (ECM)[1] and cell–cell adhesion events. The cytoskeleton is mechanically linked to the ECM by integrins so that cytoskeletal stiffening increases in direct proportion to applied stress (Wang et al., 1993). Integrins can therefore serve as mechanochemical transducers (Ingber, 1991). Integrins can also function as signaling receptors that transduce biochemical signals both into and out of cells (Clark and Brugge, 1995; Sjaastad and Nelson, 1997). Intracellular signals known to be linked to integrins include pH, Ca^{2+}, protein kinase C activation, and protein tyrosine phosphorylation (Schwartz et al., 1991a; Schwartz, 1993).

Integrin signaling pathways are generally believed to be initiated by integrin clustering through interactions with insoluble ECM ligands (Clark and Brugge, 1995). These signals are initiated by cell interactions with ECM-coated substrates or with beads coated with ECM proteins or antiintegrin antibodies (Miyamoto et al., 1995b; Plopper et al., 1995). When soluble ECM protein or antibody is added, minimal or no signaling is thought to occur, but if soluble antibody is followed by a cross-linking antibody, signaling pathways are activated (Yamada and Geiger, 1997). A widely studied recognition site on ECM proteins, including vitronectin (VN) and fibronectin (FN) (Schwarzbauer, 1991), is the tripeptide Arg-Gly-Asp (RGD), which is recognized by a common subset of integrins, including $\alpha_v\beta_3$, $\alpha_5\beta_1$, $\alpha_v\beta_5$, and $\alpha_{IIb}\beta_3$. RGD peptides are known to disrupt integrin-dependent cell adhesive events (Akiyama, 1996) as well as produce inhibitory effects on major cellular processes such as platelet aggregation and angiogenesis (Weiss et al., 1997). For this reason, RGD peptides are potential therapeutic agents for thrombotic diseases and cancer. One important, unresolved issue is whether RGD peptides act solely by disrupting cell–ECM contacts or whether they provide direct signals to cells by binding to unoccupied integrins. Recent data from our laboratories suggest that soluble RGD peptides may provide vasoactive signals to cells in the vascular wall (Mogford et al., 1996, 1997; D'Angelo et al., 1997). Thus, RGD peptides

---

Address all correspondence to Michael J. Davis, Department of Medical Physiology, 336 Reynolds Medical Building, Texas A & M University Health Science Center, College Station, TX 77843-1114. Tel.: (409) 845-7816. Fax: (409) 847-8635. E-mail: mjd@tamu.edu

---

1. *Abbreviations used in this paper*: ECM, extracellular matrix; F11, β_3 integrin monoclonal antibody; FAK, focal adhesion kinase; FN, fibronectin; HMα5-1, α_5 integrin monoclonal antibody; I_{Ba}, whole-cell Ba^{2+} current; MHC, anti–rat IgG monoclonal antibody; PSS, physiological saline solution; SMC, smooth muscle cell(s); VN, vitronectin.

may be capable of directly stimulating integrin-dependent intracellular signaling pathways.

In rat cremaster muscle arterioles, integrin-binding RGD peptides and fragments of denatured collagen type I cause dilation through an interaction with the $\alpha_v\beta_3$ integrin on vascular smooth muscle (Mogford et al., 1996). Dilation is associated with a decrease in intracellular Ca^{2+} concentration ($[Ca^{2+}]_i$) (D'Angelo et al., 1997) and can be prevented by a function-blocking antibody specific for the β_3 integrin (Mogford et al., 1996). In addition to these prolonged effects, RGD peptides also cause a transient, endothelium-independent constriction of arterioles, mediated by the $\alpha_5\beta_1$ integrin (Mogford et al., 1997). In rat afferent arterioles, RGD peptide causes a sustained constriction that is associated with an increase in smooth muscle cell $[Ca^{2+}]_i$ (Yip and Marsh, 1997). The signaling mechanisms downstream from integrin-ligand binding are poorly understood, particularly in vascular smooth muscle cells (SMCs). We hypothesized that the L-type, voltage-gated calcium channel was involved in the vasoactive responses of arterioles since this channel is known to be a major pathway for calcium entry into vascular SMCs. To test this hypothesis, we isolated single SMCs from rat cremaster arterioles and selectively measured whole-cell calcium current before and after application of integrin ligands in both soluble and insoluble form.

Materials and Methods

Cell Isolation Techniques

Male Sprague-Dawley rats (120–200 g) were anesthetized with intraperitoneal injection of pentobarbital sodium (120 mg/kg). All animal handling procedures followed institutional guidelines. The two cremaster muscles were excised and pinned flat for vessel dissection in a 4°C silastic-coated Plexiglas chamber containing Ca^{2+}-free saline solution. The composition was (in mM) 147 NaCl, 8.6 KCl, 1.17 $MgSO_4$, 1.2 NaH_2PO_4, 5.0 D-glucose, 2.0 pyruvate, 0.02 EDTA, and 3 MOPS (pH adjusted to 7.4 with NaOH), with BSA (0.1 mg/ml; Amersham Life Science, Arlington Heights, IL) added to maintain cell integrity. Dissected segments of first- and second-order arterioles were transferred to a tube of low-Ca^{2+} saline solution containing (in mM) 144 NaCl, 5.6 KCl, 0.1 $CaCl_2$, 1.0 $MgCl_2$, 0.42 Na_2HPO_4, 0.44 NaH_2PO_4, 10 Hepes, 4.17 $NaHCO_3$, and 1 mg/ml BSA (pH adjusted to 7.4 with NaOH) at room temperature for 10 min. After allowing the vessels to settle to the bottom of the tube, the solution was decanted and replaced with low-Ca^{2+} saline containing 26 U/ml papain (Sigma Chemical Co., St. Louis, MO) and 1 mg/ml dithioerythritol (Sigma Chemical Co.). The vessels were incubated for 30 min at 37°C with occasional agitation, after which vessel fragments were transferred to low-Ca^{2+} saline solution containing 1.95 collagenase (FALGPA U/ml; Sigma Chemical Co.), 1 mg/ml soybean trypsin inhibitor (Sigma Chemical Co.), and 75 U/ml elastase (Calbiochem, La Jolla, CA) for 15 min at 37°C. After further digestion, the remaining fragments were rinsed two times with low-Ca^{2+} saline solution and gently triturated using a fire-polished Pasteur pipette to release single cells.

Patch Clamp Techniques

Perforated, whole-cell recordings were made as described previously (Rae and Fernandez, 1991). Micropipettes were pulled from 1.5-mm glass tubing (Corning No. 8161; Warner Instruments, Hamden, CT) on a programmable puller and fire polished. Pipette resistances ranged from 1 to 3 MΩ. The pipettes were dipped for 2–3 s in Cs^+ pipette solution (high Cs^+) containing (in mM) 110 CsCl, 20 TEA chloride, 10 EGTA, 2 $MgCl_2$, 10 Hepes, and 1 $CaCl_2$ (pH adjusted to 7.2 with CsOH) and then backfilled with the same solution containing 240 μg/ml amphotericin B. An EPC-7 amplifier (HEKA, Darmstadt-Eberstadt, Germany) was used to record current, and hydraulic manipulators (model M0-102; Narishige, Tokyo, Japan) were used for fine control of the micropipettes. Analog to digital

conversions were made using a TL-1 DMA interface (Axon Instruments, Foster City, CA) and stored on a Pentium computer for subsequent analysis. Data were sampled at 5–10 kHz and filtered at 1–2 kHz using an eight-pole Bessel filter. Series resistance varied from 2 to 6 MΩ. Current records were analyzed using pClamp (version 6.0.3; Axon Instruments). Currents through the L-type calcium channel were elicited by voltage ramps (from −100 mV to +80 mV, duration = 200 ms) or by voltage steps (from −80 to +60 mV in 10 mV increments, duration = 300 ms). All experiments were performed at 22°C.

A suspension of freshly dispersed cells was plated onto a thin glass coverslip in a recording chamber on the stage of an inverted microscope. The coverslip was not usually treated, but in some experiments it was coated with FN (120 kD, 20 μg/ml) before addition of cells (Schwartz, 1993). Current recordings were made from individual cells between 30 min and 3 h after plating. Cells harvested using the digestion procedure were elongated with tapered ends in physiological saline solution (PSS), refractile under interference contrast optics, and contractile in solutions containing 140 mM K^+ or 20 mM Ba^{2+}. At the beginning of each experiment, the recording chamber was suffused with PSS from a gravity-fed reservoir at a rate of 1.5 ml/min. PSS had the following composition (in mM): 136 NaCl, 5.9 KCl, 10 Hepes, 1.16 NaH_2PO_4, 1.2 $MgCl_2$, 1.8 $CaCl_2$, 18 D-glucose, 0.02 EGTA, and 2 pyruvate (pH adjusted to 7.4 with NaOH). To record whole-cell current through the calcium channel, Ba^{2+} (20 mM) was used as the charge carrier in place of K^+ and Na^+ in the bath solution. This procedure is known to increase the size of the inward currents elicited by depolarization, and to minimize calcium-dependent inactivation of these currents (Griffith et al., 1994). The Ba^{2+} bath solution (20 Ba^{2+}) contained (in mM) 20 $BaCl_2$, 124 choline chloride, 10 Hepes, and 15 D-glucose (pH adjusted to 7.4 with TEA-OH).

Both ramp and step voltage protocols elicited inward, whole-cell Ba^{2+} currents (I_{Ba}) that peaked at +30 mV (range = 3.0–10.4 pA/pF); typically, these currents were stable for more than 30 min. Since current–voltage (I-V) relations for the ramp and step protocols were nearly identical, the average of five voltage ramps was used to measure I_{Ba} in most experiments. The activation portion of the I-V curve (from −60 to +30 mV) increased smoothly to a single maximum with no secondary "hump" in its voltage dependence, which is the pattern consistent with activation of only a single type Ca^{2+} channel (L-type) in this tissue (Nelson et al., 1990; Cox et al., 1992). As noted previously (Hill et al., 1996), the entire I-V relation was shifted about 30 mV to the right in 20 mM Ba^{2+} solution. This behavior is typical for voltage-gated calcium channels because of the fact that the equilibrium potential for the permeable ion shifts to the right with increasing extracellular ion concentration. When physiological Ca^{2+} is used as the charge carrier, the peak of the I-V curve occurs between −10 mV and 0 mV, and the activation threshold occurs at approximately −50 mV, as demonstrated in other SMC preparations (Aaronson et al., 1988).
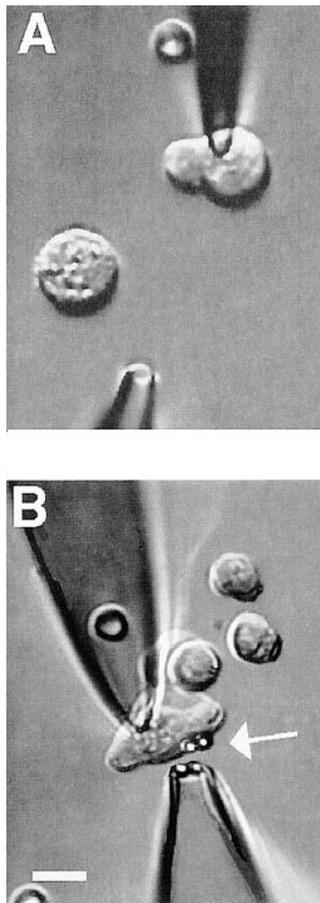
Ligand Application

VN, FN (120 kD), lyophilized cyclic GPenGRGDSPCA (cRGD, with Pen indicating penicillamine), and the control GRGESP peptide (RGE) were obtained from GIBCO-BRL (Gaithersburg, MD). The anti–β_3 integrin function-blocking antibodies (F11; anti–rat monoclonal), 2C9.G2 (monoclonal), and the anti–α_5 integrin function-blocking antibody (HMα5-1; anti–rat monoclonal raised in Armenian hamster) were obtained from PharMingen (San Diego, CA). Anti–rat MHC class I monoclonal antibody (MHC; clone R4-8B1) was obtained from Seikagaku Inc. (Tokyo, Japan). Anti–Armenian hamster monoclonal IgG was obtained from Sigma Chemical Co. Monovalent antibodies were made by digesting F11 (in stock solution) with papain, followed by subsequent extraction of Fc fragments using a column of anti–mouse Fc coupled to Sephadex. The resulting Fab digest displayed a prominent band at 50 kD with no evidence of intact F11 at 150 kD.

For application to single cells, each agent was added to 20 Ba^{2+} solution and ejected from a picospritzer pipette (General Valve Corp., Fairfield, NJ) positioned ∼50 μm away from a cell (Fig. 1 A).

Application of Protein-coated Beads

Streptavidin-coated microspheres (3.2 μm in diameter) were obtained from Bangs Laboratories (Fishers, IN). Before each experiment, the beads were coated with protein using a biotinylation procedure. Biotinylated FN, F11, VN, HMα5-1, and MHC were prepared using a method similar to that described previously (Hnatowich et al., 1987; Larson et al., 1992). The molar ratio of NHS-LC-Biotin (Pierce Chemical Co., Rockford, IL) to protein (10 μg/ml) was 20:1. To remove unreacted biotin, ul-

Figure 1. Methods for application of integrin ligands to smooth muscle cells. The images show voltage-clamped SMCs during application of (A) soluble integrin ligand from a picospritzer pipette or (B) protein-coated beads using gentle aspiration from a pipette. In both panels, the pipette at the top is a recording pipette used to hold the cell at −80 mV. Cells are contracted because of the solutions used. In A, the lower pipette is connected to a picospritzer for rapid application of solutions to the area surrounding the cell. In B, a red blood cell can be seen on the chamber bottom (underneath, not inside, the patch pipette). The pipette at the bottom is a large-tip pipette containing FN-coated beads. Two beads become attached to the cell (white arrow), and two remain in the pipette. Both panels: bath solution is 20 Ba^{2+}; patch pipette solution is high Cs^{+}; second pipette solution: 20 Ba^{2+}. Bar, 10 μm.

Figure 2. Effects of soluble cRGD on I$_{Ba}$. (A) Time course of changes in I$_{Ba}$ (measurements made at 15-s intervals) for a single arteriolar SMC in response to application of soluble cRGD peptide (100 μM). Test potential was +30 mV in each case. Individual traces at right are leak-subtracted current traces at the time points indicated by the symbols. Cell capacitance was 12 pF. (B) Bar graph summarizing data for effects of soluble cRGD (n = 9), soluble RGE (n = 4), vehicle (n = 4), and nifedipine (1 μM, n = 7). For each cell, the data represent peak currents 1 min after application, as normalized to the current at the peak of the control I-V relationship (usually +20 or +30 mV). (C) Summary I-V curves for Ba^{2+} current before or 60 s after application of soluble cRGD (100 μM). Data from nine cells. All panels: bath solution is 20 Ba^{2+}; pipette solution is high Cs^{+}; HP = −80 mV. *P < 0.05 vs. control.

trafree-MC filters were used (Millipore Corp., Bedford, MA). Nonspecific sites on the beads were blocked by incubation with 0.1% heat-denatured BSA in PSS. A dilute suspension of beads in Ba^{2+} bath solution was then used to backfill micropipettes for application to single cells. These pipettes were positioned 5–10 μm away from the cells and fashioned so that their tip diameters were approximately twice the diameter of the beads; gentle pressure from a glass syringe (<2 cm H$_2$O) was used to eject the beads (Fig. 1 B).
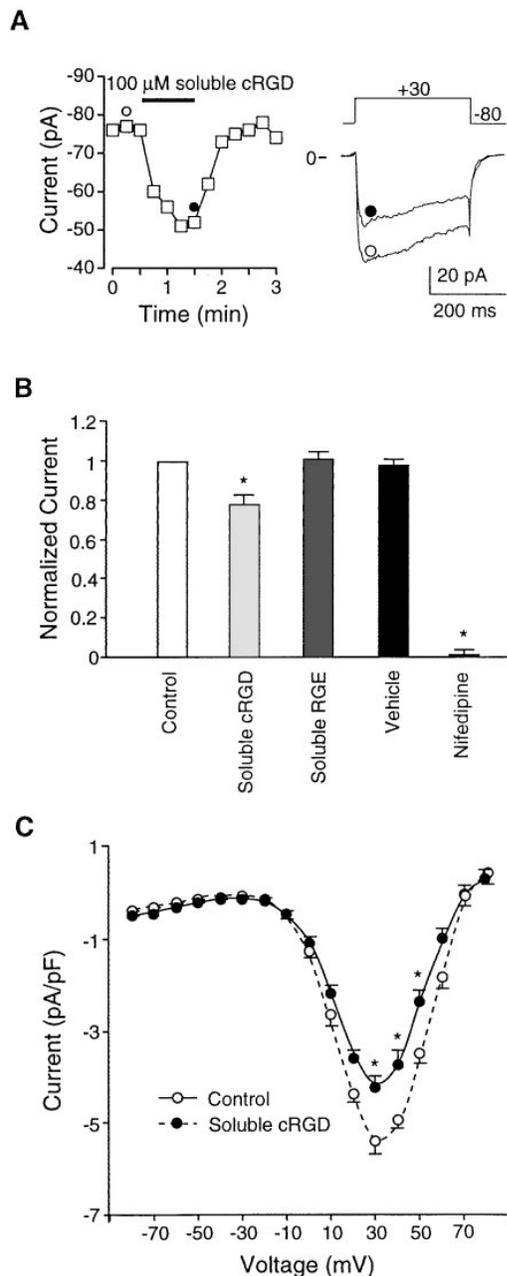
Data Analysis

Whole-cell recordings were made from cells with capacitances varying from 4 to 16 pF. We used data only from cells in which stable gigaseals were maintained. In most analyses, the raw current value was normalized to cell capacitance (an index of cell size) and expressed as current density (pA/pF). Statistical comparisons were performed with repeated-measures analysis of variance followed by post hoc tests, or with an independent two-tail t test, as appropriate. Averaged values are expressed as mean ± SEM. Values of P < 0.05 were considered to be statistically significant.

Results

Effect of cRGD on I$_{Ba}$

The effect of soluble cRGD peptide (100 μM for 1 min) on inward Ba^{2+} current is shown in Fig. 2. This dose of peptide was reported to produce near-maximal dilation of isolated cremaster arterioles (Mogford et al., 1996). Currents from single arteriolar myocytes were elicited every 15 s by a depolarizing pulse to +30 mV (300-ms duration) from a holding potential of −80 mV. The time course of the response from a representative cell is shown on the left side

of Fig. 2 *A*, and individual current traces at the indicated time points are shown on the right side. Before peptide application, peak current ranged from −76 pA to −77 pA. Within 15 s after application of soluble cRGD peptide (100 μM) from a picospritzer pipette, current was inhibited (to −60 pA) and maximal inhibition (to −51 pA) was achieved 45 s after cRGD application. Nearly complete recovery from inhibition (to −75 pA) was observed within 30 s after peptide washout.

The average response of nine cells to soluble RGD peptide is summarized in Fig. 2 *B*, where the data for each cell have been normalized to the peak Ba^{2+} current recorded just before peptide application. On average, 100 μM cRGD produced 22% inhibition of I_{Ba} at +30 mV (measurements taken immediately before peptide washout). Also illustrated in the bar graph are the effects of vehicle, RGE peptide (which does not interact with integrin receptors), and nifedipine, a dihydropyridine calcium channel blocker. Neither vehicle nor RGE peptide (80 μM; *n* = 4) had a significant effect on I_{Ba}. Nifedipine (1 mM; *n* = 7) produced nearly 100% inhibition of current at this dose, which is consistent with the behavior of an L-type Ca^{2+} channel. A comparison of current–voltage relationships recorded before and during cRGD application (Fig. 2 *C*) indicates that inhibition of I_{Ba} occurred across the entire range of voltages associated with activation of the L-type Ca^{2+} channel. Thus, there appeared to be no significant effect of RGD peptide on the threshold or reversal potential of the current.

Effect of Vitronectin on I_{Ba}

VN is known to interact with several integrins, including $\alpha_v\beta_3$ (the VN receptor). Fig. 3 *A* illustrates the effect of soluble VN on I_{Ba}. Before application, peak current in this representative cell was stable between −86 and −87 pA. Within 15 s after ejection of soluble VN (0.04 μM) from the picospritzer pipette, I_{Ba} decreased to −69 pA, with a further inhibition to −49 pA at 60 s after application. Recovery of current was complete within 60 s after VN washout. The bar graph in Fig. 3 *A* summarizes results from seven cells. On average, this concentration of soluble VN inhibited current by 39 ± 5%. Although not illustrated in this figure, inhibition of I_{Ba} by VN was sustained during longer periods of application (48 ± 7% inhibition at 4 min).

Fig. 3 *B* shows the effect of VN-coated beads on I_{Ba}. The top trace shows the time course of changes in current before (time = 0 min) and after attachment of four beads to a representative cell. Note that both peak and steady-state currents were inhibited within 1 min of bead attachment, remained inhibited for ~5 min, and then gradually returned toward control levels even though the beads appeared to remain attached. Data from six cells are summarized in the lower portion of Fig. 3 *B*. On average, a 20% inhibition of I_{Ba} was observed in response to bead attachment. As a control for nonspecific mechanical effects associated with bead application, the response to uncoated beads was also tested (*open circles*); no significant changes in I_{Ba} were noted with uncoated beads (*n* = 5) or with BSA-coated beads (*n* = 4).

Inhibition of I_{Ba} after attachment of VN-coated beads
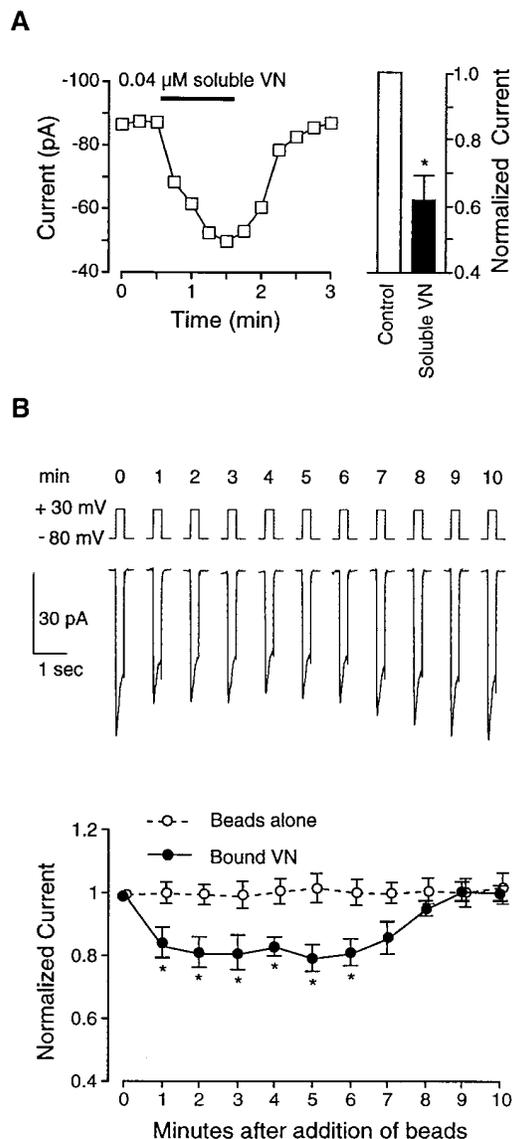
Figure 3. Effects of VN on I_{Ba}. (*A*) Graph at left shows time course of changes in I_{Ba} for a single cell before and during application of soluble VN (0.04 μM). Test potential was +30 mV in each case, and measurements were made at 15-s intervals. Cell capacitance was 15 pF. Bar graph at right shows summary data (*n* = 7) for I_{Ba} 60 s after application of soluble VN compared with control current (just before VN application). Currents were normalized to the current at the peak of the control I-V relationship. (*B*) Top traces show time course of changes in I_{Ba} (note compressed time scale for each trace compared with traces in Fig. 2 *A*) for a single cell before and after application of four VN-coated beads (at *t* = 0 min). Lower graph shows summary time course of I_{Ba} changes in response to VN-coated beads (*filled circles*; 2–5 beads/cell; *n* = 6) or uncoated beads (*open circles*; *n* = 5). All values were normalized to the peak value of I_{Ba} at *t* = 0 min. Both panels: bath solution is 20 Ba^{2+}; pipette solution is high Cs^+; HP = −80 mV. *$P < 0.05$ vs. control.

was proportional to the number of beads that attached to a given cell, a process over which we had only partial control. Regression analysis of the percent inhibition of I_{Ba} as a function of the number of attached beads gave a correlation coefficient of 0.86 ($\Delta I_{Ba} = -0.8$ pA $- 5.2 \times$ No. of

beads). For the purpose of determining the average responses of cells to coated beads in this and subsequent protocols, data were therefore pooled from cells to which between two and five beads attached.

Effect of β_3 Antibody on I_{Ba}

To test the hypothesis that the effects of cRGD and VN were mediated through the $\alpha_v\beta_3$ receptor, a function-blocking, monoclonal antibody to the rat β_3 integrin (F11) was applied to the cells. F11 is known to block the dilatory effects of cRGD peptide on isolated arterioles (Mogford et al., 1996). β_3 integrins are known to associate with two different α subunits (Hemler, 1990), but only one of those, α_v, has been identified in vascular smooth muscle (Yip and Marsh, 1997). Fig. 4 A shows the time course of changes in I_{Ba} after application of soluble F11 (0.03 μM) to a representative cell. In this cell, soluble F11 inhibited current from -70 pA to -45 pA by 1 min after application. Data from nine cells are summarized in the bar graph of Fig. 4 A and show that this dose of soluble F11 inhibited I_{Ba} by an average of $33 \pm 5\%$. We also tested the effect of a second β_3 integrin antibody, 2C9.G2, which is reported to block adhesion (Schultz and Armant, 1995). After 60 s of application, soluble 2C9.G2 (0.03 μM) inhibited I_{Ba} by $22 \pm 4.5\%$ ($n = 8$). In addition, we made Fab fragments of F11 to test the effect of a monovalent integrin ligand on Ca^{2+} current. After dilution to 0.03 μM in PSS, Fab fragments caused a $29 \pm 5\%$ inhibition of I_{Ba} 1 min after application ($n = 7$). As a control for nonspecific effects of antibody, a nonintegrin binding antibody (anti–rat MHC, 0.2 μM) was also tested; MHC had no significant effect on current ($n = 4$), as shown in the right portion of Fig. 4 A.

When F11-coated beads were applied to cells, I_{Ba} was inhibited (Fig. 4 B, closed circles). I_{Ba} was reduced to 61% of control at 1.5 min after F11 bead attachment. The inhibition lasted $\sim$5 min, after which current gradually and spontaneously returned toward control values, even though the beads remained attached. As a control for non-specific effects of antibody-coated beads, we tested the responses of cells to MHC-coated beads, which had no significant effect on I_{Ba} (Fig. 4 B, open circles).

Effect of Fibronectin on I_{Ba}

Next, we examined the effect of FN on current. FN is known to interact with both $\alpha_v\beta_3$ and $\alpha_5\beta_1$ receptors present in this cell type, as well as with a number of other integrins (Hynes, 1992). Fig. 5 A shows the time course of changes in I_{Ba} in response to soluble FN (0.1 μM). In this cell, soluble FN inhibited I_{Ba} from -80 pA to -56 pA within 60 s after application. The response of seven cells to soluble FN is summarized by the bar graph in Fig. 5 A. On average, this concentration of soluble FN reduced I_{Ba} to 75% of control at 1 min. The inhibition was maintained for at least 10 min, when current was still reduced to $80 \pm 5\%$ ($n = 5$; data not shown).

To test the effect of insoluble FN on I_{Ba}, FN-coated beads were applied to single cells. The top trace in Fig. 5 B shows the response of a representative cell to attachment of three FN-coated beads. Interestingly, FN-coated beads had the opposite effect on current compared with VN-coated beads or F11-coated beads. Attachment of FN-
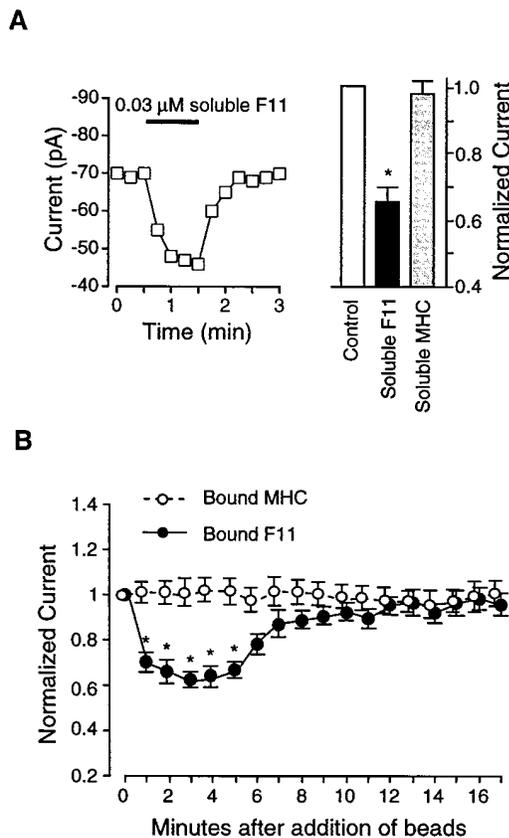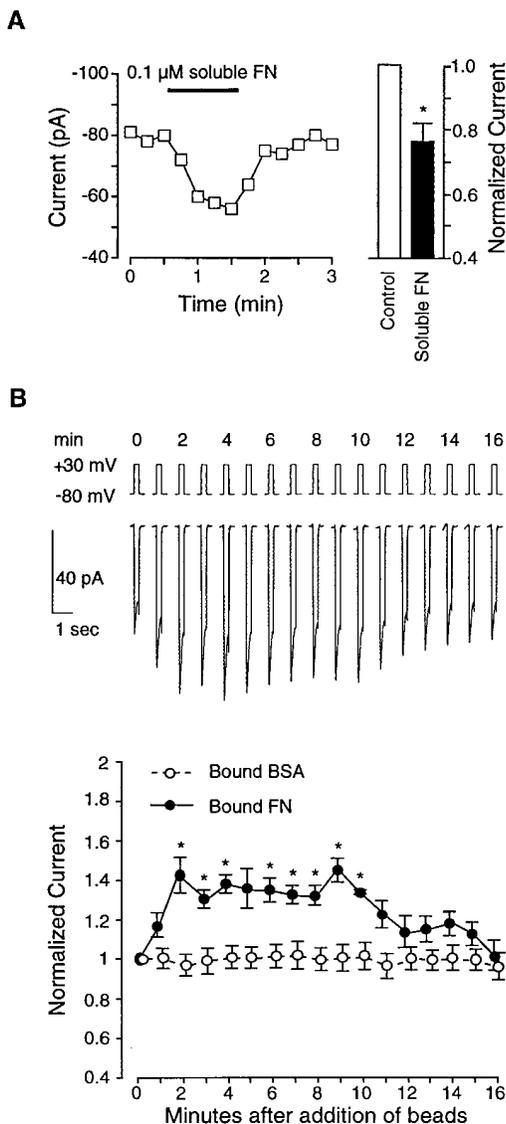
Figure 4. Effects of the β_3 antibody, F11, on I_{Ba}. (A) Graph at left shows time course of changes in I_{Ba} for a single cell before and during application of soluble F11 (0.03 μM). Test potential was $+30$ mV in each case, and measurements were made at 15-s intervals. Cell capacitance was 15 pF. Bar graph at right shows summary data for I_{Ba} 60 s after application of soluble F11 ($n = 9$) or soluble MHC (0.2 μM; $n = 4$), compared with control current. Currents were normalized to the current at the peak of the control I-V relationship. (B) Summary time course of I_{Ba} changes in response to F11-coated beads (*filled circles*; $n = 6$) or MHC-coated beads (*open circles*; $n = 9$). All values were normalized to the peak value of I_{Ba} at $t = 0$ min. Both panels: bath solution is 20 Ba^{2+}; pipette solution is high Cs^+; HP = -80 mV. *$P < 0.05$ vs. control.

coated beads led to an enhancement of I_{Ba} as early as 1 min after bead attachment. This enhancement peaked at 2 min ($\sim$135% of control), remained stable for 10 min, and then declined gradually by 16 min, even though the beads remained attached. For reference, the time course of changes in I_{Ba} in response to BSA-coated beads (which had no significant effect on current) is shown.

Effect of α_5 Antibody on I_{Ba}

The fact that insoluble VN and insoluble FN had opposite effects on current suggests that an integrin other than $\alpha_v\beta_3$ might mediate the enhancement of I_{Ba} in response to FN-coated beads. Experiments by Mogford et al. (1997) also suggest a role for the $\alpha_5\beta_1$ receptor in vasoactive responses of arterioles because RGD peptide-mediated dilation was converted to constriction after blockade of β_3 integrins:

A

B

Figure 5. Effects of FN on I_{Ba}. (*A*) Graph at left shows time course of changes in I_{Ba} for a single cell before and during application of soluble FN (0.1 μM). Test potential was +30 mV in each case, and measurements were made at 15-s intervals. Cell capacitance was 12 pF. Bar graph at right shows summary data (*n* = 7 cells) for I_{Ba} 60 s after application of soluble FN, compared with control current (just before FN application). Currents were normalized to the current at the peak of the control I-V relationship. (*B*) Top traces show time course of changes in I_{Ba} for a single cell before and after application of three FN-coated beads (at *t* = 0 min). Lower graph shows summary time course of I_{Ba} changes in response to FN-coated beads (*filled circles; n* = 9) or BSA-coated beads (*open circles*; *n* = 4). All values were normalized to the peak value of I_{Ba} at *t* = 0 min. Both panels: bath solution is 20 Ba²⁺; pipette solution is high Cs⁺; HP = −80 mV. *$P <$ 0.05 vs. control.

the steady-state portion of that constriction was mediated by endothelin and blocked by α_5 antibody, but the initial transient constriction was an endothelium-independent response.

To test for the involvement of the $\alpha_5\beta_1$ integrin in our preparation, we used the anti–rat α_5 antibody, HMα5-1. The α_5 subunit is known to associate only with β_1, making this antibody specific for the $\alpha_5\beta_1$ heterodimer (Hynes, 1992). Fig. 6 *A* shows the effect of applying soluble HMα5-1 to a representative cell: no significant change in I_{Ba} was observed. The bar graph in Fig. 6 *A* summarizes the response of nine cells to application of soluble HMα5-1, which on average produced less than a 2% change in I_{Ba}.

However, when beads coated with HMα5-1 were applied to cells, a large and significant increase in I_{Ba} was consistently observed, as summarized in Fig. 6 *B* (*left*). Within the first minute after attachment of α_5-coated beads, I_{Ba} had increased to 158% of control. I_{Ba} peaked at 170% of control ∼3 min after bead application and then progressively declined toward control; however, I_{Ba} did not completely recover even by 17 min after α_5-coated bead attachment. Individual current recordings before and after HMα5-1 application are shown in Fig. 6 *B* (*right*). The two sets of tracings represent currents evoked from a holding potential of −80 mV (*top*) or −40 mV (*bottom*) before and after attachment of HMα5-1–coated beads. As is evident from these recordings, the current stimulated by HMα5-1 was completely inhibited by nifedipine (1 μM), which is consistent with the conclusion that it flowed through L-type calcium channels. Although there is no selective blocker of T-type calcium channels, the possibility that some current might be contributed by T-type channels is ruled out by the fact that the time course of the current recordings evoked from the two different holding potentials are virtually identical.
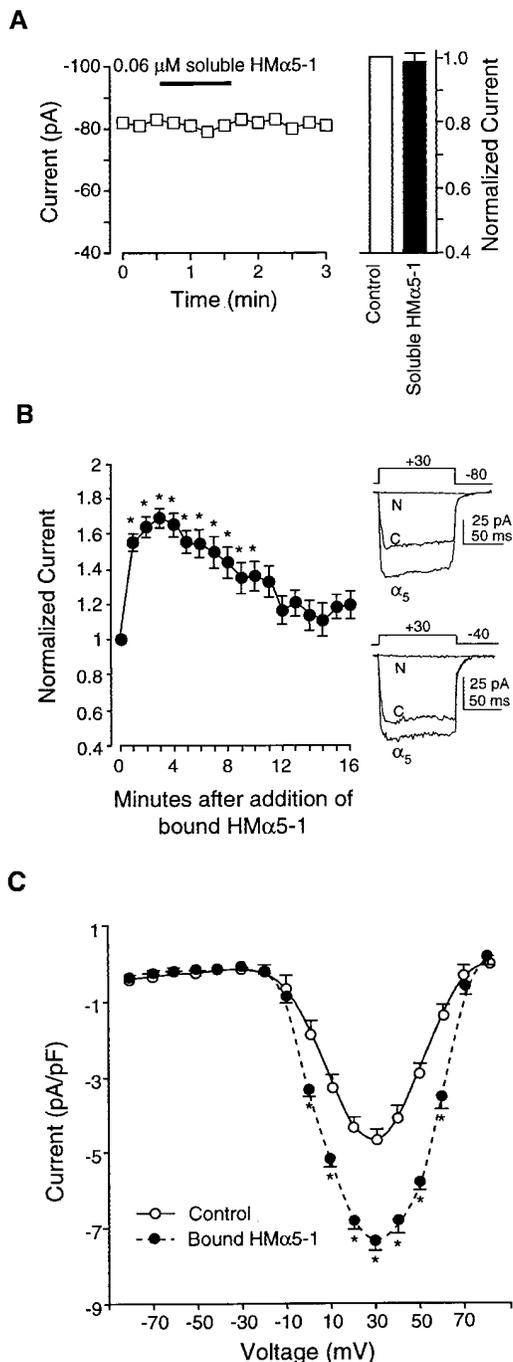
Fig. 6 *C* compares the current–voltage relationships for control current and current stimulated by bound HMα5-1. There appeared to be no significant effect on either the threshold or reversal potential of the current.

Effect of Antibody Pretreatment on I_{Ba} Response to Coated Beads

To test the idea that clustering of receptors was required to initiate signaling through the $\alpha_5\beta_1$ integrin, soluble α_5 antibody was first applied to cells, and then anti–hamster IgG was subsequently added. As shown in Fig. 7 *A*, there was no response to either agent alone, but when both agents were applied in combination, a significant enhancement in current was noted. The time course of this enhancement was approximately the same as that seen in response to insoluble α_5 antibody (compare to Fig. 6 *B*).

If the response of arteriolar smooth muscle cells to FN-coated beads involves interaction of insoluble FN with both $\alpha_v\beta_3$ and $\alpha_5\beta_1$ integrins, we predicted that pretreatment with antibody specific to one integrin would result in changes in current characteristic of selective activation of the other integrin. To test this hypothesis, cells were treated with either F11 to block β_3 or HMα5-1 to block α_5 before application of FN-coated beads. Fig. 7, *B–D*, shows the results of these experiments.

In Fig. 7 *B*, application of soluble F11 caused a 30% inhibition of I_{Ba}, an effect which is comparable to that observed previously (compare to Fig. 4 *A*). From this new baseline, application of FN-coated beads increased current from 70% of control to 116% of control. Although interpretation of this response is complicated by the shift in

baseline, the absolute change in I_{Ba} appeared to be larger than that observed in response to FN-coated beads alone (average increase = 35%; Fig. 5 B) and nearly as large as that produced by insoluble HMα5-1 (Fig. 6 B).

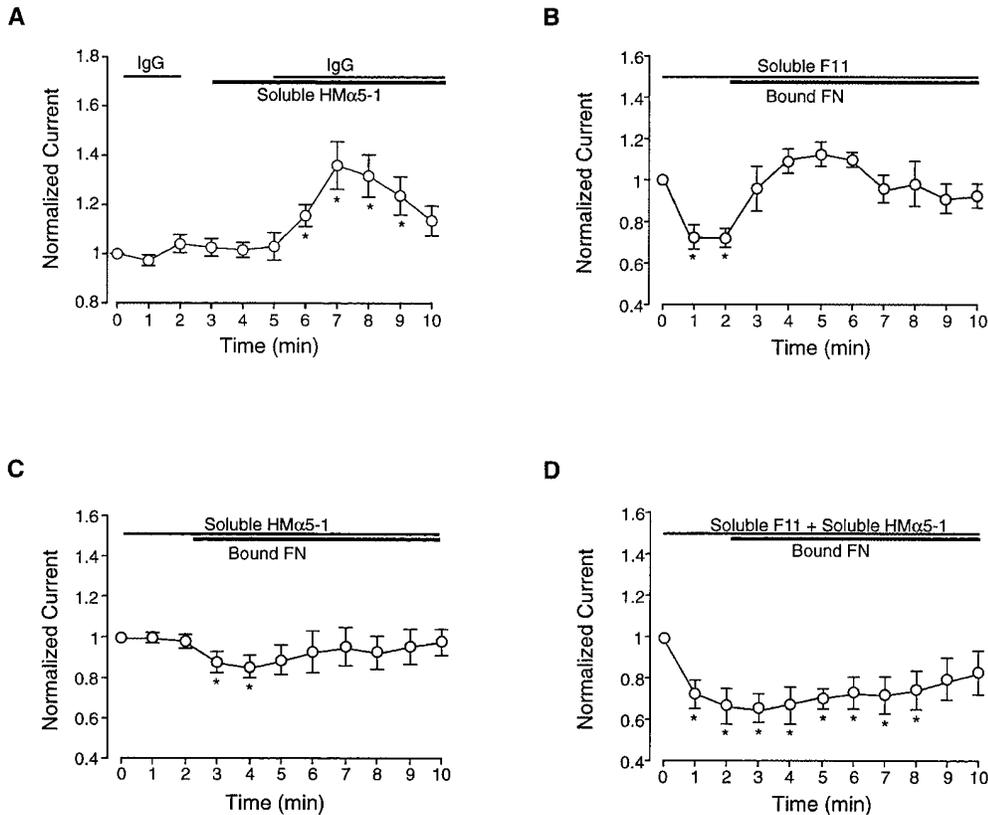In Fig. 7 C, application of soluble HMα5-1 again produced no change in I_{Ba}, but subsequent application of FN-coated beads caused a significant inhibition of current, which is the opposite response observed to FN-coated beads alone (Fig. 5). This observation is consistent with the hypothesis that insoluble FN activates both β_3 and α_5 integrins in these cells. Importantly, it also indicates that soluble HMα5-1 was indeed interacting with the $\alpha_5\beta_1$ receptor even though no change in I_{Ba} was noted in response to soluble HMα5-1 alone. Interestingly, simultaneous application of F11 and HMα5-1 resulted in a 34 ± 8% decrease in current ($n = 5$), and little change in current was noted after subsequent application of FN-coated beads (Fig. 7 D).

Discussion

To investigate the mechanisms underlying the vasoactive effects of ECM proteins and integrin-specific peptides on rat skeletal muscle arterioles (Mogford et al., 1996, 1997), we measured the response of L-type Ca^{2+} channel current in arteriolar myocytes to integrin ligands. Soluble $\alpha_v\beta_3$ ligands (cRGD, VN, FN, bivalent or monovalent β_3 antibodies) caused significant inhibition of calcium current, as did beads coated with VN or β_3 antibody. In contrast, beads coated with $\alpha_5\beta_1$ ligands (FN or α_5 antibody) caused significant enhancement of current. Soluble α_5 antibody alone had no effect on current but blocked the increase in current evoked by FN-coated beads and enhanced current when applied in combination with an appropriate IgG. This is the first electrophysiological evidence for regulation of a Ca^{2+} channel by integrin–ligand interactions and demonstrates that $\alpha_v\beta_3$ and $\alpha_5\beta_1$ integrins in smooth muscle are differentially linked through intracellular signaling pathways to the L-type calcium channel.

The implications of our findings are threefold: (a) part of the resting current through L-type Ca^{2+} channels in vascular smooth muscle, and therefore blood vessel tone, is dependent on integrin-matrix interactions; (b) bidirectional regulation of Ca^{2+} influx in this cell type can be achieved through preferential ligation of $\alpha_v\beta_3$ or $\alpha_5\beta_1$ integrins; (c) soluble integrin ligands can initiate signaling through the $\alpha_v\beta_3$ receptor. Since ECM protein denaturation and fragmentation can provide soluble integrin-specific signals to cells (Davis, 1992), this mechanism is likely to be important in the microvascular response to injury (Mogford et al., 1996). Inhibition of smooth muscle cell Ca^{2+} current could account for integrin-mediated vasodilation of arterioles (Mogford et al., 1996).

Figure 6. Effects of the α_5 antibody, HMα5-1, on I_{Ba}. (*A*) Left trace shows time course of changes in I_{Ba} for a single cell before and during application of soluble HMα5-1 (0.06 μM). Test potential was +30 mV in each case, and measurements were made at 15-s intervals. Cell capacitance was 8 pF. Bar graph at right shows summary data for I_{Ba} 60 s after application of soluble HMα5-1 ($n = 9$), compared with control current. Currents were normalized to the current at the peak of the control I-V relationship. (*B*) Left graph shows time course of average I_{Ba} changes in response to HMα5-1–coated beads ($n = 5$). HMα5-1–coated beads caused a biphasic change in I_{Ba} with a large, significant increase lasting about 4 min, followed by a slow return toward control while the beads remained attached. All values were normalized to the peak value of I_{Ba} at $t = 0$ min. Right traces show current traces evoked by a depolarizing pulse to +30 mV from a holding potential of −80 mV (*top*) or −40 mV (*bottom*). C, control; α5, HMα5-1-coated beads attached; *N*, HMα5-1–coated beads attached in the presence of nifedipine (1 μM). (*C*) I-V curve for currents before (*control*) or 4 min after attachment of HMα5-1–coated beads. All panels: bath solution is 20 Ba^{2+}; pipette solution is high Cs^+; *$P <$ 0.05 vs. control.

Figure 7. Effects of antibody pretreatment on response to coated beads. (*A*) Enhancement in current (*n* = 5) is observed during application of soluble HMα5-1 in combination with anti–Armenian hamster IgG. Neither IgG or soluble HMα5-1 alone altered current, but when both were added in combination, current was enhanced over approximately the same time course as with bound HMα5-1. (*B*) Time course of change in I_{Ba} when FN-coated beads were applied to cells in the presence of soluble F11 (0.03 μM; *n* = 7). Currents are normalized to the value of I_{Ba} at *t* = 0 min. Soluble F11 failed to inhibit the enhancement in I_{Ba} after bead attachment, although it inhibited current alone, as in Fig. 4 *A*. In fact, the magnitude of the change in current after FN bead attachment was greater than in the absence of F11 (Fig. 5 *B*) and similar to that observed in response to HMα5-1–coated beads (Fig. 6 *B*). (*C*) Time course of change in I_{Ba} when FN-coated beads were applied to cells after application of soluble HMα5-1 (0.06 μM; *n* = 12). Soluble HMα5-1 alone had no effect on current but blocked the rise in current after FN bead attachment; in fact, a slight but significant decrease in current was observed. (*D*) Time course of change in I_{Ba} when FN-coated beads were applied to cells after pretreatment with soluble HMα5-1 (0.06 μM) and soluble F11 (0.03 μM) in combination. An initial decrease in current was observed (presumably due to the effect of F11), and very little change in current was seen after application of insoluble FN. All panels: bath solution is 20 Ba^{2+}; pipette solution is high Cs^+; HP = −80 mV. *$P < 0.05$ vs. control.

Integrin Signaling in Response to Tissue Injury

Local vasodilation is one of the initial responses to tissue injury, resulting in an increase in blood flow to the affected area. This response is mediated primarily by arterioles, which are the strategic control point for local regulation of pressure and flow in every tissue. Increased flow contributes to injury repair by enhancing delivery of inflammatory cells to the injured site. Classic mediators of injury-induced arteriolar dilation include reactive oxygen species (Wei et al., 1981), tachykinins, and histamine (Treede et al., 1990). Recently, Mogford et al. (1996) described an additional mechanism by which RGD-containing peptides induce vasodilation by interacting with the $\alpha_v\beta_3$ integrin on smooth muscle cells of rat skeletal muscle arterioles. Involvement of the $\alpha_v\beta_3$ integrin was implicated by the findings that (*a*) cRGD and GRGDSP peptide were more potent vasodilators than GRGDNP peptide (enhancement of RGD potency by cyclization implicates the involvement of α_v integrins [Pierschbacher and Ruoslahti, 1987]) and (*b*) dilations were attenuated in the presence of a function-blocking β_3 monoclonal antibody (Mogford et al., 1996). In addition to synthetic peptides, fragments of denatured collagen type I were potent vasodilators of arterioles (Mogford et al., 1996). While RGD sequences are

not exposed in native collagen, cryptic RGD sites become exposed after collagen denaturation and proteolysis, allowing for their interaction with RGD-binding integrins. Exposure of cryptic RGD sites has been proposed to be a potential wound recognition signal during tissue injury (Davis, 1992). Thus, a certain proportion of the $\alpha_v\beta_3$ receptors may normally be unoccupied on vascular smooth muscle, and after tissue injury, generation of RGD peptide signals that bind the receptor result in decreased Ca^{2+} current, arteriolar dilation, and increased blood flow to the injured tissue.

Arteriolar dilations to RGD-containing peptides and proteins are mediated by direct effects on vascular smooth muscle integrins rather than on endothelial cell integrins (Mogford et al., 1996). However, none of the downstream signaling mechanisms in smooth muscle have been identified, except that dilation to soluble cyclo-RGD peptide is preceded by a significant decrease in smooth muscle $[Ca^{2+}]_i$ (D'Angelo et al., 1997). Our finding that cRGD caused an inhibition of current through the L-type Ca^{2+} channel in the same cell type (Fig. 2) is consistent with data from intact vessels. In isolated arterioles (Mogford et al., 1996; D'Angelo et al., 1997), dilation was the result of inhibition of myogenic tone, which in resistance vessels

(Nelson et al., 1990; Hill and Meininger, 1994) is dependent on basal influx of Ca^{2+} through L-type Ca^{2+} channels and can be antagonized by dihydropyridines (Hill and Meininger, 1994). We confirmed that the dihydropyridine nifedipine completely blocked current in our cells (Figs. 2 B and 6 B). Mogford et al. (1996) found that cRGD peptide also inhibited phenylephrine- and KCl-induced vascular tone, but the primary actions of both agents are known to be mediated by Ca^{2+} influx through voltage-gated Ca^{2+} channels as well (Nelson et al., 1988).

Integrin-mediated $[Ca^{2+}]_i$ Signaling

Integrin-mediated $[Ca^{2+}]_i$ signaling has been demonstrated in a number of cell types, including endothelium (Schwartz and Denninghoff, 1994) and vascular smooth muscle (McNamee et al., 1993). Integrins including $\alpha_{IIb}\beta_3$, $\alpha_v\beta_6$, $\alpha_v\beta_5$, $\alpha_5\beta_1$, and $\alpha_v\beta_3$ (Hynes, 1992) are known to be involved in $[Ca^{2+}]_i$ signaling responses; these integrins also recognize the RGD sequence common to many ECM (FN, osteopontin, and collagens) and plasma proteins (FN, VN, and fibrinogen). Thus, our finding that Ca^{2+} channel current (and by direct extension Ca^{2+} influx [Ganitkevich and Isenberg, 1991]) is modulated after $\alpha_v\beta_3$ and $\alpha_5\beta_1$ receptor ligation is consistent with previous reports in the literature.

Changes in $[Ca^{2+}]_i$ initiated by integrin ligation involve a number of mechanisms that result in Ca^{2+} release from intracellular stores and/or Ca^{2+} influx (McNamee et al., 1993; Somogyi et al., 1994; Sjaastad et al., 1996). In endothelial cells, α_v integrins mediate a rise in $[Ca^{2+}]_i$ after adhesion to FN (Schwartz and Denninghoff, 1994). The mechanism underlying this response was not determined, but $[Ca^{2+}]_i$ increases did not occur in the absence of extracellular Ca^{2+}. Likewise, both Ca^{2+} release and Ca^{2+} influx contributed to the $[Ca^{2+}]_i$ rise after adhesion of MDCK cells to RGD-coated beads (Sjaastad et al., 1996), but the influx component was more important for feedback regulation of integrin-mediated adhesion. No mechanism for integrin-mediated Ca^{2+} influx in nonexcitable cells has been identified, although a role for a 50-kD integrin-associated protein, not yet characterized electrophysiologically, has been postulated (Brown, 1993; Schwartz et al., 1993).

Our data represent the first electrophysiological evidence that integrin ligation can modulate a plasma membrane Ca^{2+} channel. To make these measurements, Ba^{2+} was used instead of Ca^{2+} to carry current through the L-type Ca^{2+} channel because (*a*) Ba^{2+} is more permeable than Ca^{2+} through this channel, resulting in larger current; (*b*) Ba^{2+} blocks the large, outward K^+ current that normally masks Ca^{2+} current in these cells; and (*c*) Ba^{2+} currents do not exhibit the rapid inactivation observed when Ca^{2+} is used (Griffith et al., 1994). Nifedipine, a dihydropyridine that is a selective antagonist of L-type calcium channels (as opposed to other types of voltage-gated calcium channels [Birnbaumer et al., 1994]) at concentrations less than 10^{-5} M, produced essentially a complete block of basal Ca^{2+} current (Fig. 2 B) as well as inhibited the enhanced current in response to insoluble α_5-antibody (Fig. 6 B).

Although we have not directly measured $[Ca^{2+}]_i$ in our preparation, it is highly likely that any treatment causing a significant change in I_{Ba} would lead to a similar directional change in $[Ca^{2+}]_i$; this relationship has been clearly demonstrated for visceral (Ganitkevich and Isenberg, 1991) and vascular (Fleischmann et al., 1994) smooth muscle. The previously reported decrease in arteriolar smooth muscle $[Ca^{2+}]_i$ in response to soluble RGD peptide (D'Angelo et al., 1997) is consistent with inhibition of I_{Ba} by soluble RGD peptide (Fig. 2). In another vascular bed, RGD peptide caused a constriction that was associated with an increase in SMC $[Ca^{2+}]_i$ (Yip and Marsh, 1997).

The direct effect of cRGD, VN, FN, and F11 on Ca^{2+} channel current in isolated SMCs provides strong support for the concept that interaction of $\alpha_v\beta_3$ with soluble ligands transduces an intracellular signal in this cell type. It remains to be determined if $\alpha_v\beta_3$ expressed in other cell types, such as endothelium, delivers a similar or different signal. However, endothelial cells (with one exception [Bossu et al., 1989]) lack voltage-gated calcium channels and, in some ways, use opposite mechanisms of controlling calcium entry than smooth muscle. Therefore, it is not surprising that ligation of β_3 integrins might lead to increases in endothelial cell $[Ca^{2+}]_i$ (Schwartz and Denninghoff, 1994) but opposite changes in SMC $[Ca^{2+}]_i$.

Effects of Soluble and Insoluble Integrin Ligands on Ba^{2+} Current

A number of possible explanations may account for the differences between the effects of soluble and insoluble integrin ligands on Ca^{2+} channel current. An obvious possibility is that inhibition of current by soluble FN may be mediated by competitive antagonism of existing integrin–matrix interactions, as suggested for other systems (Poole and Watson, 1995). This would require constitutive phosphorylation of the channel through an integrin-dependent pathway. Indeed, the L-type calcium channel in vascular smooth muscle has been shown to require tyrosine phosphorylation for normal function (Wijetunge et al., 1992; Wijetunge and Hughes, 1996), but whether integrins regulate this pathway is not known. If they do, then disruption of existing integrin–matrix interactions by soluble ligands would produce inhibition of current while clustering of receptors by insoluble ligands (Altieri et al., 1990; Schwartz, 1993), including antibodies (Miyamoto et al., 1995*a*), would produce enhancement of current. In our system, soluble ligands of the $\alpha_v\beta_3$ receptor did produce inhibition of current; however, insoluble β_3 ligands (VN and F11) also produced inhibition of current (Figs. 3 and 4). Thus, it seems likely that these effects resulted from activation of a signaling pathway rather than competition for existing β_3–matrix interactions. Likewise, since insoluble α_5 caused enhancement of current, the competition hypothesis would predict that soluble α_5 should reduce current, which it did not.

A more tenable explanation for our results is the possibility that $\alpha_v\beta_3$ and $\alpha_5\beta_1$ integrins provide distinct and opposing signals to regulate calcium current. As illustrated in Fig. 8 *A*, we propose that selective ligands of the $\alpha_v\beta_3$ receptor (F11, 2C9.G2, VN) cause inhibition of current, selective ligands of the $\alpha_5\beta_1$ receptor (HMα5-1) cause enhancement of current, and ligands for both receptors (FN)

cause an intermediate response. Our hypothesis requires that several conditions be met: (*a*) β_1 and β_3 integrins must signal through different mechanisms in smooth muscle cells. This is supported by the different responses of current to selective ligands of the two respective integrins (Fig. 4 *B* vs. Fig. 6 *B*). In endothelial cells as well (Leavesley et al., 1993), β_1 and β_3 integrins play different roles in regulating Ca^{2+} entry (Leavesley et al., 1993). Our hypothesis also requires that (*b*) the $\alpha_5\beta_1$ integrin can only be activated by insoluble ligands. This is consistent with the observation that soluble α_5 antibody had no effect on current (Fig. 6 *A*), yet was an effective blocker of the response to insoluble FN (Fig. 7 *C*). Experiments by other groups have also shown that soluble α_5 antibody failed to increase pH_i unless it was cross-linked with a secondary antibody to induce integrin clustering (Schwartz et al., 1991*b*). Our hypothesis requires that (*c*) the $\alpha_v\beta_3$ integrin must be capable of signaling when ligands are supplied in either a soluble or insoluble form. In support of this is the observation that six different soluble β_3 ligands (cRGD, VN, FN, bivalent F11, monovalent F11, and 2C9.G2 antibody) all caused inhibition of I_{Ba}, as did two different insoluble β_3 ligands (VN and F11). According to our hypothesis, (*d*) soluble signals must be transmitted only through the $\alpha_v\beta_3$ integrin and not the $\alpha_5\beta_1$ integrin. This is supported by the observation that soluble FN (a proposed ligand only for $\alpha_v\beta_3$) inhibited current, while insoluble FN (a known ligand for both $\alpha_v\beta_3$ and $\alpha_5\beta_1$) enhanced current. Finally, our hypothesis predicts that (*e*) selective ligands of the $\alpha_5\beta_1$ receptor should produce a larger enhancement in current than a common ligand for both integrins (Fig. 8 *B*). Accordingly, the magnitude of the increased current was nearly twofold greater when cells were presented with α_5 antibody–coated beads compared with FN-coated beads (compare Figs. 5 and 6). Collectively, our data are consistent with the hypothesis that $\alpha_v\beta_3$ ligation leads to inhibition of the Ca^{2+} channel, whereas $\alpha_5\beta_1$ ligation leads to stimulation of the Ca^{2+} channel. Further work will be needed to thoroughly test this hypothesis and to determine if other integrins in vascular smooth muscle are also linked to this channel.

Mechanisms of Calcium Current Modulation

The mechanisms by which $\alpha_v\beta_3$ and $\alpha_5\beta_1$ ligands modulate this calcium channel are not yet clear, but the possibility that the ligands exert a direct effect on the channel seems unlikely for several reasons: (*a*) selective antibodies for β_3 and α_5 integrins modulate Ca^{2+} current, suggesting that regulation occurs in a signaling pathway upstream from the channel rather than at the channel itself; (*b*) there is no reported RGD binding sequence in the structure of α_{1c}, the L-type subunit found in vascular smooth muscle (Koch et al., 1990); and (*c*) antagonists such as dihydropyridines inhibit Ca^{2+} channels within seconds, and divalent cations block within a fraction of a second (Dolphin, 1995; Hughes, 1995), while inhibition of current by soluble $\alpha_v\beta_3$ ligands (Figs. 2–5) required ∼60 s to achieve >90% of its maximal effect.

In terms of mechanisms, a more likely possibility is that modulation of current after integrin ligation involves clustering of integrin receptors, recruitment of cytoskeletal
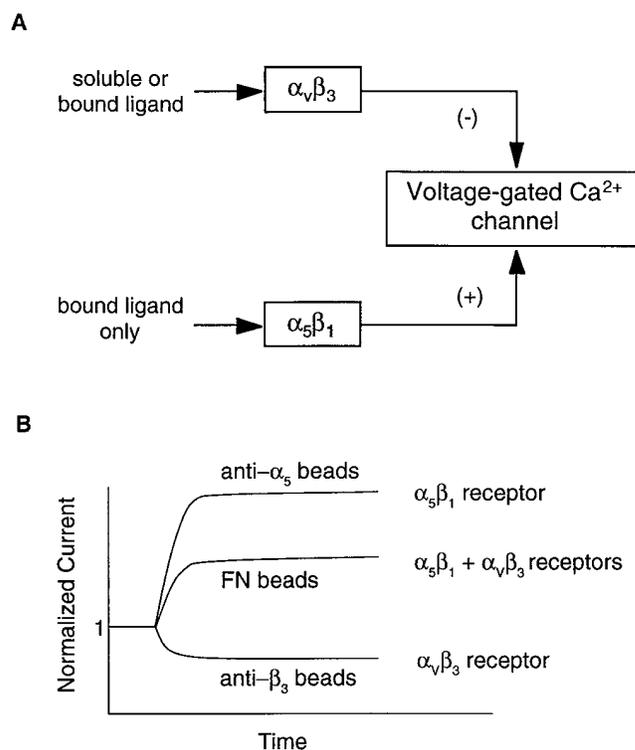

Figure 8. Diagram of hypothesized interactions between $\alpha_v\beta_3$ and $\alpha_5\beta_1$ integrins and the voltage-gated Ca^{2+} channel in vascular smooth muscle. See Discussion for details.

proteins, and tyrosine phosphorylation of cytoplasmic signaling molecules, such as FAK, Src, or paxillin, as they are brought into close proximity (Clark and Brugge, 1995). One difference between the effects of soluble and insoluble ligands in our experiments is that soluble ligands had sustained effects on current (soluble FN inhibited current for at least 10 min), while insoluble ligands elicited changes in current that lasted between 6 and 14 min followed by spontaneous recovery. The latter observation would be consistent with a phosphorylation-dependent signaling step that is subject to negative feedback control. This could occur at the level of the receptor, at the channel, or at an intermediate step. In this regard, the affinity of the $\alpha_5\beta_1$ integrin for ligand has been shown to be controlled by the Ca^{2+}-dependent phosphatase CaMKII (Bouvard et al., 1998), such that inhibition of CaMKII preserves the high affinity state of $\alpha_5\beta_1$. A link between integrin signaling and CaMKII has also been demonstrated in vascular smooth muscle (Bilato et al., 1997). Activation of CaMKII after Ca^{2+} influx through L-type channels could reduce $\alpha_5\beta_1$ affinity and reverse the enhancement of current stimulated by $\alpha_5\beta_1$ ligation. However, other possibilities for initiating signals downstream from integrin ligation may also exist, including pathways involving phospholipase C and protein kinase C (Somogyi et al., 1994).

It is likely that $\alpha_v\beta_3$ and $\alpha_5\beta_1$ integrins associate directly with one of the L-type Ca^{2+} channel subunits (e.g., α_{1c}) or with another protein that controls gating or modulates channel activity. A number of cytoplasmic signaling molecules are potential candidates to interact with the calcium

channel. Data from recent experiments on the L-type Ca^{2+} channel in visceral smooth muscle (Hu et al., 1998) have shown that PDGF, which activates a receptor tyrosine kinase, enhances L-type Ca^{2+} current and this effect is blocked after dialysis of the cells with anti-FAK or anti-Src antibodies. Furthermore, α_{1c} coprecipitates with c-Src in that tissue and has a potential tyrosine phosphorylation site (Koch et al., 1990). Dialysis of SMCs with c-Src (Wijetunge and Hughes, 1995) or with a peptide that activates c-Src (Wijetunge and Hughes, 1996) results in enhancement of Ca^{2+} current. Taken together, these results and our own preliminary data showing that tyrosine kinase inhibitors reverse the enhancement of current in response to insoluble FN (Wu, X., G.A. Meininger, G.E. Davis, J.E. Mogford, S.H. Platts, and M.J. Davis. 1997. *Microcirculation.* 4:136a) suggest that the pore-containing subunit of the L-type Ca^{2+} channel may be tyrosine phosphorylated by c-Src, which in turn is regulated by integrin ligation. Additional experiments will be needed to directly test this idea.

References

Aaronson, P.I., T.B. Bolton, R.J. Lang, and I. MacKenzie. 1988. Calcium currents in single isolated smooth muscle cells from the rabbit ear artery in normal-calcium and high-barium solutions. *J. Physiol.* 405:57–75.

Akiyama, S.K. 1996. Integrins in cell adhesion and signaling. *Hum. Cell.* 9:181–186.

Altieri, D.C., W.L. Wiltse, and T.S. Edgington. 1990. Signal transduction initiated by extracellular nucleotides regulates the high affinity ligand recognition of the adhesive receptor CD11b/CD18. *J. Immunol.* 145:662–670.

Bilato, C., K.A. Curto, R.E. Monticone, R.R. Pauly, A.J. White, and M.T. Crow. 1997. The inhibition of vascular smooth muscle cell migration by peptide and antibody antagonists of the $\alpha_v\beta_3$ integrin complex is reversed by activated calcium/calmodulin-dependent protein kinase II. *J. Clin. Invest.* 100: 693–704.

Birnbaumer, L., K.P. Campbell, W.A. Catterall, M.M. Harpold, F. Hofmann, W.A. Horne, Y. Mori, A. Schwartz, T.P. Snutch, T. Tanabe, and R.W. Tsien. 1994. The naming of voltage-gated calcium channels. *Neuron.* 13:505–506.

Bossu, J.L., A. Feltz, J.L. Rodeau, and F. Tanzi. 1989. Voltage-dependent transient calcium currents in freshly dissociated capillary endothelial cells. *FEBS Lett.* 255:377–380.

Bouvard, D., A. Molla, and M.R. Block. 1998. Calcium/calmodulin-dependent protein kinase II controls $\alpha_5\beta_1$ integrin–mediated inside-out signaling. *J. Cell Sci.* 111:657–665.

Brown, E.J. 1993. Signal transduction from leukocyte integrins. *In* Cell Adhesion Molecules. M.E. Hemler and E. Mihich, editors. Plenum Press, New York. 105–125.

Clark, E.A., and J.S. Brugge. 1995. Integrins and signal transduction pathways: the road taken. *Science.* 268:233–239.

Cox, R.H., D. Katzka, and M. Morad. 1992. Characteristics of calcium currents in rabbit portal vein myocytes. *Am. J. Physiol.* 263:H453–H463.

D'Angelo, G., J.E. Mogford, G.E. Davis, M.J. Davis, and G.A. Meininger. 1997. Integrin-mediated reduction in vascular smooth muscle $[Ca^{2+}]_i$ induced by RGD-containing peptide. *Am. J. Physiol.* 272:H2065–H2070.

Davis, G.E. 1992. Affinity of integrins for damaged extracellular matrix: $\alpha_v\beta_3$ binds to denatured collagen type I through RGD sites. *Biochem. Biophys. Res. Commun.* 182:1025–1031.

Dolphin, A.C. 1995. Voltage-dependent calcium channels and their modulation by neurotransmitters and G proteins. *Exp. Physiol.* 80:1–36.

Fleischmann, B.K., R.K. Murray, and M.I. Kotlikoff. 1994. Voltage window for sustained elevation of cytosolic calcium in smooth muscle cells. *Proc. Natl. Acad. Sci. USA.* 91:11914–11918.

Ganitkevich, V.Y., and G. Isenberg. 1991. Depolarization-mediated intracellular calcium transients in isolated smooth muscle cells of guinea-pig urinary bladder. *J. Physiol.* 435:187–205.

Griffith, W.H., L. Taylor, and M.J. Davis. 1994. Whole-cell and single-channel calcium currents in guinea pig basal forebrain neurons. *J. Neurophysiol.* 71: 2359–2376.

Hemler, M.E. 1990. VLA proteins in the integrin family: structures, functions, and their role on leukocytes. *Annu. Rev. Immunol.* 8:365–400.

Hill, M.A., and G.A. Meininger. 1994. Calcium entry and myogenic phenomena in skeletal muscle arterioles. *Am. J. Physiol.* 267:H1085–H1092.

Hill, M.A., M.J. Davis, J.B. Song, and H. Zou. 1996. Calcium dependence of indolactam-mediated contractions in resistance vessels. *J. Pharmacol. Exp. Ther.* 276:867–874.

Hnatowich, D.J., F. Virzi, and M. Ruschowski. 1987. Investigations of avidin and biotin for imaging applications. *J. Nucl. Med.* 28:1294–1302.

Hu, X.-Q., N. Singh, D. Mukhopadhyay, and H.I. Akbarali. 1998. Modulation of voltage-dependent Ca^{2+} channels in rabbit colonic smooth muscle cells by c-Src and focal adhesion kinase. *J. Biol. Chem.* 273:5337–5342.

Hughes, A.D. 1995. Calcium channels in vascular smooth muscle cells. *J. Vasc. Res.* 32:353–370.

Hynes, R.O. 1992. Integrins: versatility, modulation, and signaling in cell adhesion. *Cell.* 69:11–25.

Ingber, D. 1991. Integrins as mechanochemical transducers. *Curr. Opin. Cell Biol.* 3:841–848.

Koch, W.J., P.T. Ellinor, and A. Schwartz. 1990. cDNA cloning of a dihydropyridine-sensitive calcium channel from rat aorta. Evidence for the existence of alternatively spliced forms. *J. Biol. Chem.* 265:17786–17791.

Larson, R.C., G.G. Ignotz, and W.B. Currie. 1992. Effect of fibronectin on early embryo development in cows. *J. Reprod. Fert.* 96:289–297.

Leavesley, D.I., M.A. Schwartz, M. Rosenfeld, and D.A. Cheresh. 1993. Integrin β_1- and β_3-mediated endothelial cell migration is triggered through distinct signaling mechanisms. *J. Cell Biol.* 121:163–170.

McNamee, H.P., D.E. Ingber, and M.A. Schwartz. 1993. Adhesion to fibronectin stimulates inositol lipid synthesis and enhances PDGF-induced inositol lipid breakdown. *J. Cell Biol.* 121:673–678.

Miyamoto, S., S.K. Akiyama, and K.M. Yamada. 1995*a*. Synergistic roles for receptor occupancy and aggregation in integrin transmembrane function. *Science.* 267:883–885.

Miyamoto, S., H. Teramoto, O.A. Coso, J.S. Gutkind, P.D. Burbelo, S.K. Akiyama, and K.M. Yamada. 1995*b*. Integrin function: molecular hierarchies of cytoskeletal and signaling molecules. *J. Cell Biol.* 131:791–805.

Mogford, J.E., G.E. Davis, S.H. Platts, and G.A. Meininger. 1996. Vascular smooth muscle $\alpha_v\beta_3$ integrin mediates arteriolar vasodilation in response to RGD peptides. *Circ. Res.* 79:821–826.

Mogford, J.E., G.E. Davis, and G.A. Meininger. 1997. RGDN peptide interaction with endothelial $\alpha_5\beta_1$ integrin causes sustained endothelin-dependent vasoconstriction of rat skeletal muscle arterioles. *J. Clin. Invest.* 100:1647–1653.

Nelson, M.T., N.B. Standen, J.E. Brayden, and J.F. Worley III. 1988. Noradrenaline contracts arteries by activating voltage-dependent calcium channels. *Nature.* 336:382–385.

Nelson, M.T., J.B. Patlak, J.F. Worley, and N.B. Standen. 1990. Calcium channels, potassium channels, and voltage dependence of arterial smooth muscle tone. *Am. J. Physiol.* 259:C3–C18.

Pierschbacher, M.D., and E. Ruoslahti. 1987. Influence of stereochemistry of the sequence Arg-Gly-Asp-Xaa on binding specificity in cell adhesion. *J. Biol. Chem.* 262:17294–17298.

Plopper, G.E., H.P. McNamee, L.E. Dike, K. Bojanowski, and D.E. Ingber. 1995. Convergence of integrin and growth factor receptor signaling pathways within the focal adhesion complex. *Mol. Biol. Cell.* 6:1349–1365.

Poole, A.W., and S.P. Watson. 1995. Regulation of cytosolic calcium by collagen in single human platelets. *Br. J. Pharmacol.* 115:101–106.

Rae, J.L., and J. Fernandez. 1991. Perforated patch recordings in physiology. *NIPS (News Physiol. Sci.).* 6:273–277.

Schultz, J.F., and D.R. Armant. 1995. β_1- and β_3-class integrins mediate fibronectin binding activity at the surface of developing mouse peri-implantation blastocysts. *J. Biol. Chem.* 270:11522–11531.

Schwartz, M.A. 1993. Spreading of human endothelial cells on fibronectin or vitronectin triggers elevation of intracellular-free calcium. *J. Cell Biol.* 120: 1003–1010.

Schwartz, M.A., and K. Denninghoff. 1994. α_v integrins mediate the rise in intracellular calcium in endothelial cells on fibronectin even though they play a minor role in adhesion. *J. Biol. Chem.* 269:11133–11137.

Schwartz, M.A., D.E. Ingber, M. Lawrence, T.A. Springer, and C. Lechene. 1991*a*. Multiple integrins share the ability to induce elevation of intracellular pH. *Exp. Cell Res.* 195:533–535.

Schwartz, M.A., C. Lechene, and D.E. Ingber. 1991*b*. Insoluble fibronectin activates the Na/H antiporter by clustering and immobilizing integrin $\alpha_5\beta_1$, independent of cell shape. *Proc. Natl. Acad. Sci. USA.* 88:7849–7853.

Schwartz, M.A., E.J. Brown, and B. Fazeli. 1993. A 50 kDa integrin-associated protein is required for integrin-regulated calcium entry in endothelial cells. *J. Biol. Chem.* 268:19931–19934.

Schwarzbauer, J.E. 1991. Fibronectin: from gene to protein. *Curr. Opin. Cell Biol.* 3:786–791.

Sjaastad, M.D., and W.J. Nelson. 1997. Integrin-mediated calcium signaling and

regulation of cell adhesion by intracellular calcium. *BioEssays.* 19:47–55.

Sjaastad, M.D., R.S. Lewis, and W.J. Nelson. 1996. Mechanisms of integrin-mediated calcium signaling in MDCK cells: regulation of adhesion by IP$_3$- and store-independent calcium influx. *Mol. Biol. Cell.* 7:1025–1041.

Somogyi, L., Z. Lasic, S. Vukicevic, and H. Banfic. 1994. Collagen type IV stimulates an increase in intracellular Ca^{2+} in pancreatic acinar cells via activation of phospholipase C. *Biochem. J.* 299:603–611.

Treede, R.D., R.A. Meyer, K.D. Davis, and J.N. Campbell. 1990. Intradermal injections of bradykinin or histamine cause a flare-like vasodilation in monkey: evidence from laser Doppler studies. *Neurosci. Lett.* 115:201–206.

Wang, N., J.P. Butler, and D.E. Ingber. 1993. Mechanotransduction across the cell surface and through the cytoskeleton. *Science.* 260:1124–1127.

Wei, E.P., H.A. Kontos, W.D. Dietrich, J.T. Povlishock, and E.F. Ellis. 1981. Inhibition by free radical scavengers and by cyclooxygenase inhibitors of pial arteriolar abnormalities from concussive brain injury in cats. *Circ. Res.* 48:95–103.

Weiss, D.J., O.A. Evanson, and R.E. Wells. 1997. Evaluation of arginine-gly-cine-aspartate-containing peptides as inhibitors of equine platelet function. *Am. J. Vet. Res.* 58:457–460.

Wijetunge, S., and A.D. Hughes. 1995. pp60$^{c\text{-}src}$ increases voltage-operated calcium channel currents in vascular smooth muscle cells. *Biochem. Biophys. Res. Commun.* 217:1039–1044.

Wijetunge, S., and A.D. Hughes. 1996. Activation of endogenous c-Src or a related tyrosine kinase by intracellular (PY)EEI peptide increases voltage-operated calcium channel currents in rabbit ear artery cells. *FEBS Lett.* 399:63–66.

Wijetunge, S., C. Aalkjaer, M. Schachter, and A.D. Hughes. 1992. Tyrosine kinase inhibitors block calcium channel currents in vascular smooth muscle cells. *Biochem. Biophys. Res. Commun.* 189:1620–1623.

Yamada, K.M., and B. Geiger. 1997. Molecular interactions in cell adhesion complexes. *Curr. Opin. Cell Biol.* 9:76–85.

Yip, K.P., and D.J. Marsh. 1997. An Arg-Gly-Asp peptide stimulates constriction in rat afferent arteriole. *Am. J. Physiol.* 273:F768–F776.